
VeriSparse: Training Verified Locally Robust Sparse Neural Networks from Scratch

Sawinder Kaur Yi Xiao Asif Salekin
Syracuse University

Abstract

Several safety-critical applications such as self-navigation, health care, and industrial control systems use embedded systems as their core. Recent advancements in Neural Networks (NNs) in approximating complex functions make them well-suited for these domains. However, the compute-intensive nature of NNs limits their deployment and training in embedded systems with limited computation and storage capacities. Moreover, the adversarial vulnerability of NNs challenges their use in safety-critical scenarios. Hence, developing sparse models having robustness guarantees while leveraging fewer resources during training is critical in expanding NNs' use in safety-critical and resource-constrained embedding system settings. This paper presents 'VeriSparse'—a framework to search verified locally robust sparse networks starting from a random sparse initialization (i.e., scratch). VeriSparse obtains sparse NNs exhibiting similar or higher verified local robustness, requiring one-third of the training time compared to the state-of-the-art approaches. Furthermore, VeriSparse performs both structured and unstructured sparsification, enabling storage, computing-resource, and computation time reduction during inference generation. Thus, it facilitates the resource-constraint embedding platforms to leverage verified robust NN models, expanding their scope to safety-critical, real-time, and edge applications. We exhaustively investigated VeriSparse's efficacy and generalizability by evaluating various benchmark and application-specific datasets across several model architectures.

1 Introduction

Neural networks have been instrumental in transforming many real-world applications. However, *two significant hurdles* prevent their broad utilization in real-world, safety-critical, and resource-constrained settings: the compute-heavy nature of complex NN models and the lack of guarantee of adversarial robustness.

Extensive Resource Requirement. Complex NNs require significant computing resources and memory for inference and training, which can be a challenge for embedded systems and other resource-constrained environments [57, 72]. Furthermore, in real-time applications, such as real-time video processing, and hazard detection, the speed of inference becomes critical, and complex NN models deployed on resource-constrained platforms may not be able to deliver results promptly.

Adversarial Vulnerability. NNs are vulnerable to small deviations in the input, i.e., imperceptible adversarial perturbation ε , which can lead to inaccurate inferences [13]. Such vulnerability may have catastrophic effects [41] in safety-critical real-world applications such as medical diagnosis or autonomous driving, where the input data may often be slightly changed due to sensor noise, measurement errors, or adversarial attacks.

To address such vulnerability, state-of-the-art works [52, 51] have leveraged adversarial training to achieve (adversarial) robustness, which enhances NNs' ability to maintain accuracy and robustness even when the input data is slightly perturbed. The empirical adversarial training relies on finding adversarial perturbations around individual samples leveraging existing adversarial attacks and training the NNs on them. However, it cannot guarantee that no other (yet unknown) attacks would find adversarial samples. For e.g., recent approaches [64, 77] have proposed adversarial training leveraging

PGD attacks [26] of varying strengths. However, Tjeng et al. [61] showed that PGD does not necessarily generate the perturbations with maximum loss; thus, the models trained to minimize PGD adversarial loss are still vulnerable to other stronger attacks.

On the contrary, **verified local robustness** training [24, 14, 75, 69] guarantees the non-existence of adversarial samples in the vicinity of the benign samples, making it essential for safety-critical systems. Detailed background on verified local robustness training is in Section 2.

Model Compression - A Necessity. The enormous number of parameters present in dense NNs challenge their deployment in resource-constrained platforms such as self-navigation, hazard detection, etc., making it essential to generate sparser NN models. Most existing works that focus on obtaining sparse NN models aim to maintain the prediction (benign/standard) accuracy of the sparse model comparable to the dense models trained with the same objective [2, 78]. Recently, works are aiming at the additional target of adversarial robustness for a certain attack alongside standard accuracy [52, 28]. However, only two works we know addressed achieving sparse networks exhibiting high verified local robustness [52, 23]. Both followed the *train-and-sparsify mechanism* to attain sparsification (discussed in Section 2.4.1), which comprised three steps: training a dense NN to convergence with the same objective, identifying a pruning mask to remove the least important parameters, and re-training the retained parameters of the sparse NN to improve verified local robustness; which requires significant training time and resources.

To address this resource-and-time-overhead in the *train-and-sparsify* sparsification mechanism, recent literature has presented dynamic-mask-based sparse-training, i.e., *Dynamic Sparse Training (DST)* paradigms [5, 32, 8], that have successfully trained sparse networks with high prediction (standard) accuracy from scratch. DST approaches start from a sparse NN architecture (initialized with random connections and parameter weights) and allows the sparse connectivity to evolve dynamically by learning new connections and parameter weights simultaneously during training based on gradient information while keeping the number of total parameters in the sparse NN fixed. DST-based approaches extract sparse networks comparable to dense NNs in standard accuracy in significantly less training time [6]. To our knowledge, extraction of sparse NN comparable in *verified local robustness* to its dense counterpart from scratch using DST is yet to be addressed.

Problem Statement: *This work addresses the task of obtaining sparse NN from scratch, which exhibit similar standard accuracy and verified local robustness (definition is provided in section 2.2) as its dense NN counterparts while using significantly fewer parameters (1% of the comparable verified locally robust dense networks evaluated in literature).*

The paper presents **VeriSparse**, which, starting from scratch, dynamically explores and identifies the sparse network structure and parameters with the objective of obtaining high verified local robustness. Such dynamic exploration enables obtaining highly sparse networks, having *generalizability* comparable to their dense counterparts. In this work, we refer to *model generalizability* as the ability of the model to project high standard accuracy and verified local robustness simultaneously. **VeriSparse** addresses the hurdles mentioned above through simultaneously (1) reducing the NN training time and resources by starting from scratch and leveraging DST; (2) reducing the NN inference time and resources by achieving significant sparsity (using 1% of original parameters); and (3) achieving high *verified local robustness*.

The paper’s tasks and contributions are summarized below:

1. This is the first paper to demonstrate that verified locally robust sparse neural networks can be trained from scratch, comparable in *generalizability* to their dense counterparts.
2. Our preliminary analysis identified that the verification approach, CROWN-IBP [75] implicitly imposes regularization during verified local robustness training (discussed in Section 3.3.4). Leveraging the CROWN-IBP bounding mechanism and implicit regularization in the learning objective, this paper presents a DST-based approach named **VeriSparse** that trains verified locally robust sparse NNs comparable in *generalizability* to their dense counterparts from scratch.
3. Training from scratch through DST is impactful since compared to the two aforementioned *train-and-sparsify* mechanism-based baselines [52, 23], **VeriSparse** extracts sparse NNs taking 2 – 3 times less training time in the same platform. Such reduction in training time is in line with the

literature showing DST learns faster [6, 58]. Reduced training time and resources are significant in embedded systems and platforms.

4. The presented **VeriSparse** extracts both structured-pruned and unstructured-pruned sparse networks; however, it can be extended to any pruning mechanism. Compared to the baseline works [52, 23], **VeriSparse** extracted sparse NNs exhibit similar and significantly higher *generalizability* on unstructured-pruned and structured-pruned sparsed architectures. Discussion about unstructured-pruned and structured-pruned sparsed architectures are in Sections 2.4.2 and 3.3.3.
5. Our evaluation shows that the inference time of the sparse models obtained via **VeriSparse**'s unstructured pruning mechanism is *five times* lesser, on average, than their dense counterparts on NVIDIA RTX A6000, which is a computation platform optimized to leverage fine-grained sparsity [40].
6. Structured-pruned sparse NN architectures require significantly less space and inference time than their dense counterparts, even in generic computation platforms [46, 43]. According to our evaluation on the resource constraint generic computation platform, Google Pixel 6, **VeriSparse** extracted structured-pruned sparse NNs take about 5 – 8 times less memory and 2 – 5 times less inference time compared to their dense counterparts. **VeriSparse**'s structured-pruned sparsed NNs' higher *generalizability* than the baselines [52, 23], and such models' significant reduction in inference time and memory utilization makes **VeriSparse** highly impactful for resource constraint applications such as in embedded systems.
7. Our empirical study demonstrates that **VeriSparse** is applicable to both image and non-image domains and is shown to perform effectively on benchmark datasets (CIFAR-10, MNIST, & SVHN), application-relevant *Pedestrian Detection* [37] dataset, sentiment analysis NLP dataset SST-2 [56], and model architecture combinations used in the literature.

Additionally, Section 2 provides relevant backgrounds and related work discussion, and Section 5 discusses the impact, limitations and future-work scope of this study. The Appendix includes some additional results and observations.

2 Background and Related-Works

2.1 Background on Formal robustness verification

An NP-Complete problem: The complexity and the need for non-linear activation functions in recent NNs to learn complex decision boundaries makes the problem of formal robustness verification of NNs non-convex and NP-Complete [24, 55].

Relaxation based Methods: To address the challenge, Katz et al. [24] used relaxation of ReLU activations, temporarily violating the ReLU semantics, resulting in an efficient query solver for NNs with ReLU activations. The piece-wise linearity of the ReLU activations is the basis for this relaxation. Linear Relaxation based Perturbation Analysis (LiRPA) based methods compute linear relaxation of a model containing general activation functions which are not necessarily piece-wise linear and verify non-linear NNs in polynomial time. Thus, LiRPA based methods use Forward (IBP [14]), Backward (CROWN [76], Fastened-CROWN [34], α -CROWN [70], β -CROWN [63], DeepPoly [53], BaB Attack [71]) or Hybrid (CROWN-IBP [75]) bounding mechanisms to compute linear relaxation of a model. CROWN [76] uses a backward bounding mechanism to compute linear or quadratic relaxation of the activation functions. IBP [14] is a forward bounding mechanism that propagates the perturbations induced to the input towards the output layer in a forward pass based on interval arithmetic, resulting in ranges of values for each class in the output layer. CROWN-IBP [75] is a hybrid approach that demonstrated that IBP can produce loose bounds, and in order to achieve tighter bounds, it uses IBP [14] in the forward bounding pass and CROWN [76] in the backward bounding pass to compute bounding hyperplanes for the model. CROWN-IBP has been shown to compute tighter relaxations, thus, providing the better results for formal verification.

Specifically, for a sample x_0 , the perturbation neighborhood is defined as ℓ_p -ball of radius ε [76]:

$$\mathbb{B}_p(x_0, \varepsilon) := \{x \mid \|x - x_0\|_p \leq \varepsilon\}. \quad (1)$$

LiRPA aims to compute linear approximations f^ε of the model \mathcal{M}_θ (θ represents model parameters), and provide lower f_L^ε and upper f_U^ε bounds at the output layer, such that for any sample $x \in \mathbb{B}_p(x_0, \varepsilon)$ and each class j , the model output is guaranteed to follow:

$$f_L^\varepsilon(x)^j \leq \mathcal{M}_\theta(x)^j \leq f_U^\varepsilon(x)^j. \quad (2)$$

2.2 Background on Verified local robustness.

A NN model, \mathcal{M}_θ is said to be verified locally robust [12] for a sample (x_0, y) if: $\forall x \in \mathbb{B}_p(x_0, \varepsilon) \Rightarrow \mathcal{M}_\theta(x) = \mathcal{M}_\theta(x_0)$, that is, for all the samples $x \in \mathbb{B}_p(x_0, \varepsilon)$, the model is guaranteed to assign the same class as it assigns to x_0 . LiRPA approaches measure the local robustness in terms of a margin vector $m(x_0, \varepsilon) = C f^\varepsilon(x_0)$, where C is a *specification matrix* of size $n \times n$ and n is the number of all possible classes [14, 76, 75, 69]. Zhang et al. [75] defines C for each sample (x_0, y) as:

$$C_{i,j} = \begin{cases} 1, & j = y \text{ and } i \neq y \text{ (truth class)} \\ -1, & i = j \text{ and } i \neq y \text{ (other classes)} \\ 0, & \text{otherwise.} \end{cases} \quad (3)$$

The entries in matrix C depend on the true class y . In matrix C , the row corresponding to the true class contains 0 at all the indices. All the other rows, contain 1 at index corresponding to the true class ($j = y$) and -1 at index corresponding to current class ($j = i$) and 0 at all the other indices. Thus, the i^{th} value of $m(x_0, \varepsilon)$ is given by $m^i(x_0, \varepsilon) = f^\varepsilon(x_0)^y - f^\varepsilon(x_0)^i$, which is the difference of output values of the true class y from the output value corresponding to class i .

Further, $\underline{m}(x_0, \varepsilon)$ represents the lower bound of the margin vector. If all the values of the $\underline{m}(x_0, \varepsilon)$ are positive, $\forall_{i \neq y} \underline{m}^i(x_0, \varepsilon) > 0$, the model \mathcal{M}_θ is said to be locally robust for sample x_0 . That implies, the model will always assign the highest output value to the true class label y if a perturbation less than or equal to ε is induced to the sample x_0 . Thus, $\forall_j \underline{m}(x_0, \varepsilon)^j > 0$ implies the guaranteed absence of any adversarial sample in the region of interest. Furthermore, to specify the region bounded by $\mathbb{B}_p(x_0, \varepsilon)$, we use $p = \infty$ because ℓ_∞ -norm covers the largest region [66] around a sample and is most challenging and widely-used [65, 23, 67].

2.3 Background on Model training to maximize local robustness

Since, a model is considered verified locally robust for a sample (x_0, y) if all the values of $\underline{m}(x_0, \varepsilon) > 0$, the training schemes proposed by previous approaches [14, 75] aim to maximize robustness of a model by maximizing the lower bound $\underline{m}(x_0, \varepsilon)$. Xu et al. [69] defines the training objective as minimizing the maximum cross-entropy loss between the model output $\mathcal{M}_\theta(x)$ and the true label y among all samples $x \in \mathbb{B}_p(x_0, \varepsilon)$ (eq. 6 in [69]). Thus, the training loss is defined as:

$$\mathcal{L}_{\text{train}}(\mathcal{M}_\theta, \mathcal{D}, \varepsilon) = \sum_{(x_0, y) \in \mathcal{D}} \max_{x \in \mathbb{B}_p(x_0, \varepsilon)} \mathcal{L}(\mathcal{M}_\theta(x), y), \quad (4)$$

where \mathcal{D} is the dataset and $(x_0, y) \in \mathcal{D}$. Intuitively, $\mathcal{L}_{\text{train}}$ is the sum of maximum cross-entropy loss in the neighborhood of each sample in \mathcal{D} for perturbation amount ε . Wong and Kolter [67] showed that the problem of minimizing $\mathcal{L}_{\text{train}}$ (as defined in 4) and the problem of maximizing $\underline{m}(x_0, \varepsilon)$ are dual of each other. Thus, *a solution that minimizes $\mathcal{L}_{\text{train}}$, maximizes the values of $\underline{m}(x_0, \varepsilon)$, hence maximizes the local robustness for the sample (x_0, y)* . Since, $x_0 \in \mathbb{B}_p(x_0, \varepsilon)$, *minimizing $\mathcal{L}_{\text{train}}$ also maximizes benign/standard accuracy, ergo maximizes generalizability altogether*.

Xu et al. [69] computes $\max_{x \in \mathbb{B}_p(x_0, \varepsilon)} \mathcal{L}(\mathcal{M}_\theta(x), y)$ which requires computing bounding hyperplanes f_U^ε and f_L^ε using one of the aforementioned LiRPA bounding techniques. Following Xu et al. [69], **VeriSparse** employs CROWN-IBP hybrid approach as the bounding mechanism to optimize $\mathcal{L}_{\text{train}}(\mathcal{M}_\theta, \mathcal{D}, \varepsilon)$ in equation (4). The perturbation amount ε is initially set to zero and gradually increases to ε_{max} according to the perturbation scheduler ε -scheduler($\varepsilon_{\text{max}}, t, s, l$) (Section 3).

2.4 Literature Review and Background on Model Compression

Several model compression approaches, such as Quantization [2], Model Distillation [19, 7], Low-Rank Factorization [47] have been proposed to reduce the computational and storage requirements of deep neural networks (DNNs). Model Sparsification (i.e., Pruning) is the most common form of model compression, which constrains the model to use only a subset of original parameters for inference [51, 78, 30, 52].

2.4.1 Model Sparsification.

Hoeffler et al. [20] categorizes the model sparsification into three categories based on the stage at which sparsification is performed. They are discussed below:

- *Train-and-sparsify* approaches [78, 51, 52] train a dense model to convergence and remove (or prune) the parameters, either in one step or iteratively, which contribute the least towards model inference. To compensate for the information lost during pruning, an additional step of fine-tuning the retained parameters is performed by associating a static binary mask with the parameters.

- The *sparsifying-during-training* mechanisms iteratively prune and fine-tunes retained parameters while gradually increasing the overall sparsity [59, 74]. Even though the training starts with a dense model, the sparsification step starts before the dense model converges and is usually cheaper than the train-and-sparsify mechanism.

- The *sparse-training* mechanism involves training a sparse network from scratch using either a *static* or a *dynamic* mask. Identifying *static* masked sparse network is motivated by *Lottery Ticket Hypothesis (LTH)* [10]. However, finding the *static* mask in LTH [11, 10] still requires a fully or partially trained dense model to start with.

Recently developed *dynamic-mask-based sparse-training* known as Dynamic Sparse Training (DST) [5, 32] approaches follow *grow-and-prune* paradigm to achieve a favorable sparse network starting from a random sparse *seed network*. Dai et al. [5] grows the model to a certain capacity and then gradually removes the connection, following a single *grow-and-prune* stride. However, recent approaches [32, 8] employ multiple repetitions of *grow-and-prune* where, in each repetition, new connections (i.e., parameters) which minimize the natural loss are added (*grow step*), and the least important connections are removed (*prune step*).

DST approaches achieve higher efficacy than the *static-mask-based sparse-training*, attributed to high gradient flow allowing the model to learn a sparse network more effectively [8].

2.4.2 Selecting the Parameters to be Removed during Sparsification:

Selection of parameters to be removed can be done based on several criteria such as the magnitude of weights [73], the norm of corresponding gradients [35], Taylor expansion [36], minimal impact on Hessian matrix [62], etc. [20]. Additionally, recent approaches associate importance scores with each parameter based on the respective training objective [52, 23], and remove the parameters with the least important scores. However, Magnitude-based pruning is the most popular mechanism [51, 78, 30, 52, 15], which removes the least magnitude parameters suggesting that the importance of a parameter is directly proportional to the magnitude of their weights. Presented **VeriSparse** exceeds state-of-the-art without any task/objective specific important score-based parameter selection mechanism, establishing that a sparse network with high verified local robustness and accuracy comparable to its dense counterpart is attainable from scratch following trivial parameter selection mechanism.

Unstructured vs Structured pruning: Unstructured pruning zeros out the parameters depending on their individual importance [52, 78], whereas structured pruning removes channels/nodes as a whole [42, 31]. It has been observed that structured pruning is effective in significantly reducing memory and inference time in generic platforms, making them highly effective in practical use [60, 46]. Moreover, selecting parameters to be removed can be made either per-layer [52] or globally [49, 54]. Literature [49, 54] suggests the higher efficacy of global pruning over layer-wise pruning. We employ global unstructured and layer-wise structured pruning (details in Section 3).

2.5 Related work to Attain a Sparse Network with highly Verified Local Robustness

Earlier approaches aimed to achieve model sparsification to retain the prediction accuracy of the sparse model [16, 30, 38, 50, 78]. The introduction of adversarial vulnerability led to the inclusion of an additional objective of adversarial robustness in the pruning literature [51, 52, 73, 22, 29].

With the recent advances in verified local robustness, to the best of our knowledge, two recent works have aimed at achieving sparse networks which exhibit verified local robustness [52, 23]. Both of them fall under the category of *train-and-sparsify*. In contrast, the **VeriSparse** belongs to the *sparse-training* type, which aims to learn a verified locally robust sparse network from scratch.

Sehwag et al. [52] (Hydra) proposed a three-step robustness-aware model training approach accounting for both adversarial robustness and verified local robustness (also known as certified robustness). The pre-train step aims to generate a robust dense model, which then undergoes prune-training to train a robustness-aware importance score for each parameter, guiding the final pruning mask. The finetuning step updates the retained weights to recover the model’s performance. Hydra sets an equal pruning ratio for all the layers to obtain the pruning mask, which ignores the fact that different layers hold different importance toward model inference.

Kang et al. [23] developed FaShapley following Hydra’s framework with the difference in the prune-training step. It iteratively and randomly removes a small fraction of parameters while training importance scores correspond to all the parameters. The update to a parameter’s importance scores is equivalent to the magnitude of the product’s weight and gradient, which is an efficient approximation for its shapely value. The final removal of weights can be done in a structured or unstructured manner based on the importance scores (Shapley values) considered globally.

This paper considers Hydra [52] and Fashapley [23] as baselines and shows their performance comparisons with **VeriSparse**.

3 Verified Locally Robust Sparse Model via Dynamic-Mask-based Sparse-training

3.1 **VeriSparse** Overview:

VeriSparse is an iterative DST paradigm, which allows examining different connections across time under the constraints of an underlying *backbone* architecture in searching for the optimal sparse network architecture which exhibit high verified local robustness. An example overview of the **VeriSparse** approach (utilizing global unstructured pruning mechanism) is shown in Figure 1. Each parameter of the *backbone network* can either be in *active* or *dormant* state based on whether or not it belongs to the sparse network at a particular instant. In Figure 1, active and dormant parameters are shown with color and grey edges, respectively. The weight of a *dormant* parameter is set to zero. The percentage of parameters that are *dormant* is the network’s current *sparsity*.

As the initial step (Figure 1(B)), a random sparse network with target sparsity (i.e., with random active parameters and corresponding parameter values) is initialized. Then, **VeriSparse** iteratively performs a gradient-based *Thickening* and a magnitude-based *Prune* Phase. In the *Thickening Phase* (Figure 1(C)), the sparse network grows, exploring new connections (i.e., making dominant parameters active) based on the gradient information with the goal of increasing verified local robustness. In the *Pruning Phase*, the least significant parameters are removed ((Figure 1(D))) to regain the desired sparsity ((Figure 1(E))). Through such iterative *thickening and pruning* phases, the **VeriSparse** explores and examines different connectivities in searching the optimal sparse network architecture and corresponding parameter values that achieve a high verified local robustness.

3.2 Problem Definition, i.e., the Learning Objective of **VeriSparse**

For a given randomly initialized backbone architecture \mathcal{M}_θ with k parameters, the objective is to train a verified locally robust sparse network $\mathcal{M}_{\theta^\downarrow}$ which uses only a subset of available parameters (of the backbone), that is, $|\theta^\downarrow|_0 = k'$ and k' is an order of magnitude times smaller than k , $k' \ll k$. The

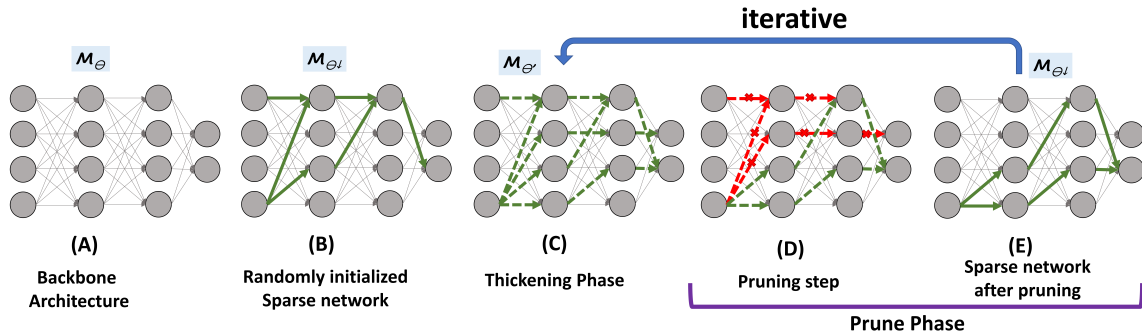


Figure 1: An illustration of the VeriSparse training utilizing the global unstructured pruning mechanism. Here, (A) The backbone \mathcal{M}_θ , which is a fully connected network; (B) The randomly initialized sparse network $\mathcal{M}_{\theta^\downarrow}$; (C) The Thickening phase where the network expand to $\mathcal{M}_{\theta'}$ within the bound of the backbone to explore new connections; Figures (D) and (E) comprise the Pruning step. In figure (D), the least important parameters are removed to regain the target sparsity, and figure (E) shows the sparsed network $\mathcal{M}_{\theta^\downarrow}$ after the pruning step. Steps (C)-(E) are iteratively performed until the sparse network with high *generalizability* is identified.

Algorithm 1 VeriSparse

Require: \mathcal{M}_θ : Backbone architecture \diamond p : Target sparsity $\in (0, 100)$ \diamond $\mathcal{D} = (X_i, y_i)_{i=1}^m$: Dataset \diamond ε_{\max} : Maximum Perturbation \diamond PM : Pruning Mechanism \diamond T : Number of training epochs \diamond (s, l) : Start and length of perturbation scheduler \diamond T -length: Length of Thickening Phase \diamond $seed$: A seed value

- 1: Randomly initialize the backbone architecture using $seed$.
- 2: $\mathcal{M}_{\theta^\downarrow} = \text{Prune}(\mathcal{M}_\theta, PM, p)$ { Prune model \mathcal{M}_θ by $p\%$ using pruning mechanism PM }
- 3: **for** epoch $t = [1, 2, \dots, T]$ **do**
- 4: $\varepsilon_t = \varepsilon$ -Scheduler($\varepsilon_{\max}, t, s, l$)
- 5: **for** minibatches $d \in \mathcal{D}$ **do**
- 6: $\mathcal{M}_{\theta'} = \underset{\theta}{\text{argmin}} \mathcal{L}_{\text{train}}(\mathcal{M}_{\theta^\downarrow}, d, \varepsilon_t)$ {Auxiliary Model $\mathcal{M}_{\theta'}$ is denser than target sparsity, i.e. $|\theta'| > |\theta^\downarrow|$ }
- 7: **end for**
- 8: **if** $t\% T$ -length == 0 **then**
- 9: $\mathcal{M}_{\theta^\downarrow} = \text{Prune}(\mathcal{M}_{\theta'}, PM, p)$ { Prune model $\mathcal{M}_{\theta'}$ by $p\%$ using pruning mechanism PM }
- 10: **end if**
- 11: **end for**

sparse model thus achieved should exhibit high accuracy and verified local robustness, comparable to a verified locally robust dense network having the same backbone architecture.

3.3 Detailed Discussion of the VeriSparse Approach

Algorithm 1 describes the VeriSparse procedure, that requires a backbone architecture \mathcal{M}_θ ; a target sparsity p ; the dataset \mathcal{D} ; the maximum perturbation ε_{\max} ; and the Pruning mechanism PM . It also requires hyperparameters that vary for different datasets and includes the number of training epochs T , the inputs for the ε -scheduler: s and l , and the length of Thickening Phase: T -length. (discussed in Section 4).

VeriSparse starts with an untrained random sparse (i.e., seed) network while keeping $p\%$ parameters of the backbone as dormant ($p = (1 - \frac{k'}{k}) \times 100$). It is an iterative procedure, and each iteration comprises two phases: • *Thickening* (lines 5 – 7 in Algorithm 1): aims to explore new parameters in the backbone resulting in lesser sparsity, and • *Pruning* (lines 8 – 10 in Algorithm 1): removes the least important parameters (i.e., based on parameter-magnitudes) to regain the target sparsity (k').

Notably, the Pruning phase is active at every " T -length" epoch, allowing the Thickening step to explore enough parameters to identify possible new network connections that may lead to a reduction in training loss $\mathcal{L}_{\text{train}}$ (i.e., improving verified local robustness). Different components and design choices of the VeriSparse approach are discussed below:

3.3.1 Seed Network (lines 1-2 in Algorithm 1)

Given a backbone architecture, a sparse seed network is computed by randomly initializing all the backbone parameters, followed by retaining $(100 - p)\%$ parameters. All the other parameters of the backbone are set to zero (made *dormant*).

3.3.2 Thickening Phase (lines 5-7 in Algorithm 1)

This phase learns the model parameters to reduce the training loss \mathcal{L}_{train} and densify the sparse network by inspecting new parameters (within the backbone). The parameter weights, including the *dormant* ones, are updated according to their corresponding gradients. This is also referred to as *gradient based growth phase* in the literature [5, 8, 32]. However, in literature [8, 32, 5], gradients are computed for the objective of maximizing standard accuracy; in contrast, **VeriSparse** aims to maximize verified local robustness of the model by minimizing the training loss \mathcal{L}_{train} as defined in Equation (4) for each mini-batch $d \in \mathcal{D}$. The perturbation ε used for computing \mathcal{L}_{train} is computed using the perturbation scheduler $\varepsilon - scheduler(\varepsilon_{max}, t, s, l)$ (in line 4 of Algorithm 1) as discussed below.

- **Perturbation Scheduler (ε -scheduler ($\varepsilon_{max}, t, s, l$)):** ε -scheduler provides a perturbation amount for every training epoch $t \geq s$, which gradually increases ε starting at epoch s . The schedule starts with a 0 perturbation and reaches ε_{max} in l epochs [14]. According to the literature [14, 75, 69], the LiRPA approaches use interval propagation arithmetic to propagate input perturbation to the output layer, where the interval size usually keeps increasing as the propagations reach deeper in the model. The gradual increase of epsilon prevents the problem of intermediate bound explosion while training; hence deems ε -scheduler necessary for effective learning. Since the bounding mechanism (to optimize equation 4) used in **VeriSparse** is CROWN-IBP [75] which is a LiRPA-based approach, the use of ε -scheduler is crucial.

- **Auxiliary Network** The updated network after the *Thickening Phase* \mathcal{M}_θ is called auxiliary network. Since there is no restriction on the capacity of the auxiliary network, it can have more than k' active parameters.

3.3.3 Pruning Phase (line 8 in 1)

The auxiliary network obtained after the *Thickening* phase needs to be compressed to the target size k' . This phase reduces the model size regarding the number of *active* parameters while having minimum impact on the *generalizability*.

This paper evaluates two magnitude-based pruning mechanisms, layer-wise structured and global unstructured pruning (which are used in baselines [52, 23]), as the pruning mechanism PM in Algorithm 1 (line 9). However, other pruning variations can also be leveraged.

- **Global Unstructured Pruning:** It considers all the model parameters (i.e., network weights) independently and removes the least significant ones concerning the whole network. **VeriSparse** employs ℓ_1 -norm-based unstructured global pruning (following [30, 44]) as the model sparsification mechanism, to attain the sparse network $\mathcal{M}_{\theta^\downarrow}$ with target size k' . Notably, ℓ_1 -norm corresponds to the magnitude of the weight of the individual parameters. Thus, **VeriSparse**'s unstructured pruning approach can be formulated as: $\theta^\downarrow = [m | m \in p^{th} \text{ percentile of } |\theta|]$,

where θ and θ^\downarrow represent parameters of the \mathcal{M}_θ and $\mathcal{M}_{\theta^\downarrow}$. It selects the highest $(100-p)\%$ parameters of \mathcal{M}_θ to form a sparse network $\mathcal{M}_{\theta^\downarrow}$ while making remaining parameters dormant. *We refer these sparse models as unstructured-pruned sparse models.*

- **Layer-wise Structured Pruning:** It considers the importance of a node/kernel as the deciding factor towards network parameter removal. All the parameters associated with the least significant nodes/kernels are removed together as groups. For structured pruning, **VeriSparse** uses ℓ_2 -norm based channel-pruning, where the ℓ_2 -norm (following [18]) of all the parameter weights corresponding to a

kernel (convolution layer) or node (linear layer) are computed to decide the indices of kernels/nodes to be pruned from a layer. Since the kernels/nodes belonging to different layers have different numbers of parameters associated with them, the norm of these kernels/nodes are not comparable globally [45]. Therefore, **VeriSparse** uses a layer-wise structured pruning approach.

Thus, if m_i represents the i th kernel/node of layer l and $m_{i,j}$ represents j^{th} parameter associated with it, structured pruning can be formulated as: $\theta_l^\downarrow = [m_i | m_i \in p_l^{\text{th}} \text{ percentile of } \sqrt{\sum_j m_{i,j}^2}]$,

where θ_l^\downarrow represents the kernel/node retained at layer l after pruning, and p_l^{th} is the pruning amount for layer l . Thus, structured pruning selects the $\lfloor (100 - p_l^{\text{th}}) \rfloor \%$ kernels or nodes in a layer, which have the highest ℓ_2 -norm of the parameters associated with them. *We refer these sparse models as structured-pruned sparse models.*

Final Step for implementation/deployment: We performed an additional step for efficient deployment for the resulting sparse network achieved through a structured pruning mechanism of **VeriSparse**. We removed the redundant nodes (the nodes having only zero weight valued parameters associated with them) using the methodology presented by Fang et al. [9]. Thus, the reduced sparse models demand fewer memory and computation time resources while exhibiting equivalent standard accuracy and robustness (Section 5). *Notably, this step does not require any further training.*

3.3.4 CROWN-IBP as the Sparse Regularizer in $\mathcal{L}_{\text{train}}$ (Algorithm 1 line 6)

Zhang et al. [75] noted that the verified local robustness training mechanism proposed by Wong and Kolter [67] and Wong et al. [68] induce implicit regularization. CROWN-IBP [75] incurs less regularization and shows an increasing trend in the magnitude of network parameters while training. However, according to our preliminary analysis, the implicit regularization caused by CROWN-IBP penalizes the network’s parameters, making them smaller compared to naturally trained networks, causing a high fraction of the parameters to be close to zero. Removal of such less significant parameters has minimal impact on model *generalizability*.

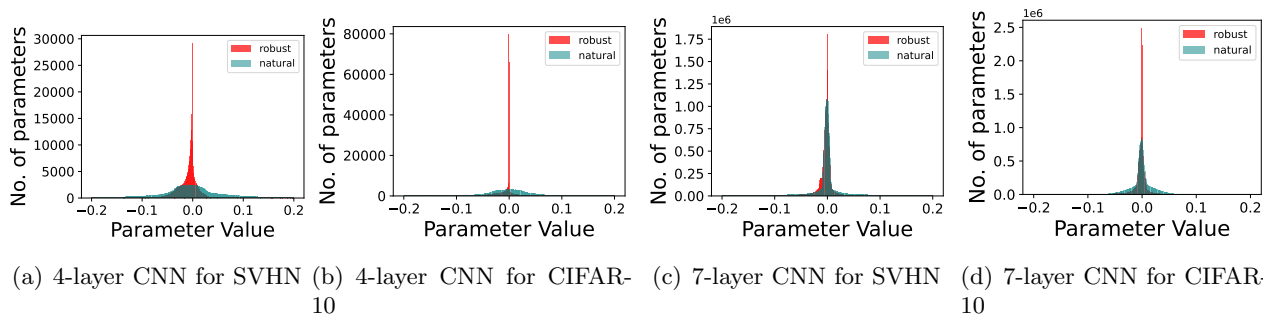


Figure 2: Weight distributions for (a) 4-layer CNN (SVHN) (b) 4-layer CNN (CIFAR-10) (b) 7-layer CNN (SVHN) (d) 7-layer CNN (CIFAR-10). The perturbation amount used for robust training is $8/255$.

For example, figure 2 shows the weight distribution of networks trained to minimize verified locally robust (CROWN-IBP [75]) and natural losses. As evident from the distribution of weights, a higher fraction of weights in verified locally robust models have very low magnitudes ($\approx 10^{-40}$).

This observation suggests that minimizing the loss $\mathcal{L}_{\text{train}}$ bounding by CROWN-IBP penalizes the network parameter magnitudes. Existing sparse training approaches [33, 17] used regularization terms in their loss function to promote sparsity. Since the $\mathcal{L}_{\text{train}}$ implicitly incorporate regularization, the **VeriSparse** (Algorithm 1 line 6) does not include any additional regularization term.

3.3.5 Learning-Rate Decay:

To enhance the effects of DST-based training, **VeriSparse** employs learning rate decay once the perturbation scheduler achieves the maximum perturbation. An initial high learning rate allows the dormant

parameters a fair chance to get considered toward the sparse structure during the *Thickeining-and-pruning* iterations.

However, as Section 4.4’s visualization suggests, the **VeriSparse** learns the sparse structure in the initial part of training, whereas in the later part, it learns the effective network parameter weights of the identified sparse network. Hence, having a decay in learning rate aid in determining the global minima in the loss space, i.e., identifying optimal parameter weights.

4 Experiments

The following section’s evaluations demonstrate **(1)** The effectiveness of **VeriSparse** in achieving verified locally robust sparse models comparable to the state-of-the-art for unstructured-pruned sparse networks and better for structured-pruned sparse networks (Section 4.1); **(2)** The scalability and generalizability of **VeriSparse** with *backbone network* (discussed in Section 3) variations, i.e., with different network complexities and architectures, such as LSTM, Resnet, ResNext and DenseNet (Section 4.2); **(3)** The applicability of **VeriSparse** to different practical application domains (Section 4.2); **(4)** the reduction in memory, training-time, and inference-time computation resource requirement through **VeriSparse** (Section 4.3); and **(5)** A visualization of the **VeriSparse**’s sparse architecture extraction and network parameter optimization dynamically. Such dynamic exploration of both network structure and parameter weights enables the effective identification of sparse networks which exhibit high verified local robustness.

Metrics for evaluations: This paper utilizes the metrics used in the previous works for formal robustness verification [52, 23] to evaluate the sparse models. The metrics are:

- *Standard Accuracy:* % of benign samples classified correctly.
- *Verified Accuracy:* % of benign samples for which all the values in the $\underline{m}(x_0, \varepsilon)$ is are positive.

Datasets and models: For a fair comparison with state-of-the-art [23], benchmark dataset CIFAR-10 [25] and SVHN [39] are used. To demonstrate the effectiveness and generalizability of **VeriSparse**, evaluations are shown for three more datasets: MNIST [27], Pedestrian Detection [37], and Sentiment Analysis SST-2 [56]. To demonstrate the versatility of the approach across different architectures, we evaluate (a) Two CNNs with varying capacity: 4-layer CNN and 7-layer CNN [14, 75]; (b) Network with skip connections: A 13-layer ResNet [68]; (c) Two DNNs: DenseNet and ResNext [69]; (d) Two sequential networks [69].

Perturbation amount: For image classification datasets, the perturbations are introduced in ℓ_p -ball of radius ε (perturbation amount), $\mathbb{B}_p(x_0, \varepsilon)$ (defined in Section 2). For a fair comparison, while comparing our results with baselines [52, 23], we use the same perturbation budget used in these works: 2/255 and 8/255 for CIFAR-10 and SVHN. For MNIST, we use a perturbation budget of 0.4, the highest perturbation amount for MNIST (i.e., most difficult scenarios) used in the literature addressing formal verification and training [14, 75, 68, 69]. For the Pedestrian Detection dataset, we use 2/255 as the perturbation amount.

For NLP dataset SST-2, the perturbations are introduced in terms of synonym-based word substitution in a sentence. Each word w has a set of synonyms $\mathbb{S}(w)$ with which it can be substituted. $\mathbb{S}(w)$ is computed using 8 nearest neighbors in counter-fitted word embedded, where the distance signifies similarity in meaning [21, 69], lesser distance implies more similarity and vice-versa. The number of words being substituted is referred to as *budget* (δ). The maximum budget used in state-of-the-art [69, 21] for formal verification is 6, and we use the same amount.

Hyperparameters: **VeriSparse** requires a set of hyperparameters as inputs: ε -scheduler inputs (T, s, l) and thickeing length T -length. T is the total number of training epochs, s is the epoch number at which the perturbation scheduler should start to increment the amount of perturbation and l specifies the length of the schedule, that is, the number of epochs in which the perturbation scheduler has to reach the maximum amount of perturbation ε_{\max} .

These values are as follows: (1) For SVHN and CIFAR-10, we use $((T, s, l) = (330, 15, 150))$, for CIFAR-10 and SVHN; (2) For MNIST, we use $((T, s, l) = (100, 10, 60))$, for CNNs and DNNs

	Model	Method	Standard	Verified	Standard	Verified
			50%		60%	
CIFAR-10	4-layer CNN Standard/ Verified at 0% 57.0/42.6	Sparsity				
		Hydra	44.2	32.5	32.5	22.0
		FaShapley	46.7	36.9	32.1	26.8
		VeriSparse	48.5	39.9	43.4	36.5
	Δ	+1.8	+3.0	+11.3	+9.7	
	7-layer CNN Standard/ Verified at 0% 66.3/47.0	Sparsity	80%		90%	
		Hydra	52.1	39.8	10.0	10.0
		FaShapley	55.5	43.9	19.5	14.2
		VeriSparse	53.1	41.9	42.5	34.6
	Δ	-2.4	-2.0	+23.0	+20.4	
SVHN	4-layer CNN Standard/ Verified at 0% 66.2/44.5	Sparsity	50%		70%	
		Hydra	47.8	33.9	19.6	19.6
		FaShapley	49.5	37.2	41.9	32.3
		VeriSparse	52.1	37.6	46.4	35.3
	Δ	+2.6	+0.4	+4.5	+3.0	
	7-layer CNN Standard/ Verified at 0% 73.8/55.4	Sparsity	80%		85%	
		Hydra	49.2	34.9	15.9	15.9
		FaShapley	60.1	43.6	39.0	32.0
		VeriSparse	64.2	46.0	58.6	42.1
	Δ	+4.1	+2.4	+19.6	+10.1	

Table 1: Standard and Verified Accuracy for 4-layer CNN and 7-layer CNN trained for CIFAR-10 and SVHN at perturbation budget $2/255$ at different sparsity amounts obtained using structured pruning. Δ represents the change than the best baseline.

(2) For LSTM trained for MNIST, we use $(T, s, l) = (20, 1, 10)$; (4) For Pedestrian Detection, the hyperparameters $(T, s, l) = (100, 20, 60)$ resulted in the models displaying the least errors empirically; and (5) For Sentiment Analysis NLP dataset (following [69]), the hyperparameters $(T, s, l) = (25, 1, 10)$ are used. Notably, using a fixed perturbation amount throughout training, results in a trivial model.

To obtain the optimum values for thickening length T -length, Optuna [1], a parameter-tuning tool, is used in order to attain the combined objective of maximizing *Standard* and *Verified* accuracy.

Also, to compute the layer-wise pruning amounts for structured pruning, we performed a grid search. We found that the optimal per-layer pruning amounts for structured pruning were similar to the ones obtained via global-unstructured pruning at the same sparsity. Thus, in this work, structured pruning leverages the layer-wise sparsities resulting from unstructured pruning to decide (i.e., grid search starting point) the pruning threshold for each model layer.

Formal verification mechanisms to compute $\mathcal{L}_{\text{train}}$ and *verified accuracy*: VeriSparse training employs CROWN-IBP [75]. In Appendix A, we show empirically that the sparse models trained using CROWN-IBP exhibit higher verified accuracy than using other bounding mechanisms such as IBP [14], CROWN [76], and Fastened-CROWN [34]. However, to be consistent with the state-of-the-art [52, 23], this section’s presented evaluations use IBP to compute *Verified accuracy*.

4.1 Establishing the effectiveness of VeriSparse: Comparison with Baselines

This section compares the sparse models obtained via VeriSparse with the state-of-the-art approaches: FaShapley [23] (best-baseline) and Hydra [52]. Notably, the code for FaShapley was made public on March 14, 2023, and was not in the final form, so we could not regenerate their results for more models and datasets. Therefore, for a fair comparison, this section’s evaluations are done with the same combination of model, dataset, and sparsity amounts as used in FaShapley [23] and compared with the baseline results as provided in their paper.

We observe a significant performance boost for sparse models obtained via the structured removal of redundant network parameters. Table 1 shows the comparison of VeriSparse with FaShapley and Hydra for two architectures: 4-layer CNN and 7-layer CNN trained for CIFAR-10 and SVHN. The perturbation amount used for training and testing these models is $2/255$. Across all model, dataset, and sparsity combinations, VeriSparse attains an average increment of 8.1% and 5.9% in *Standard* and *Verified* accuracy, respectively.

Table 2 establishes that the sparse models obtained via VeriSparse’s unstructured pruning exhibit standard and verified accuracy comparable to the FaShapley’s unstructured pruning [23]. The

	Model	Method	95%		99%		
			Standard	Verified	Standard	Verified	
CIFAR-10	4-layer CNN Standard/ Verified at 0% 57.0/42.6	Hydra	49.5	40.0	34.6	29.5	
		FaShapley	53.6	43.2	47.0	37.7	
		VeriSparse	51.7	43.3	48.2	40.4	
		Δ	-1.9	+0.1	+1.2	+2.7	
	7-layer CNN Standard/ Verified at 0% 66.3/47.0	Hydra	57.8	46.2	47.7	39.4	
		FaShapley	60.3	47.5	60.0	46.6	
		VeriSparse	62.5	50.3	59.8	47.3	
		Δ	+2.2	+2.8	-0.2	+0.7	
	SVHN	4-layer CNN Standard/ Verified at 0% 66.2/44.5	Hydra	53.0	36.7	19.6	19.6
			FaShapley	61.6	41.7	53.2	39.0
VeriSparse			59.0	43.2	51.0	38.2	
Δ			-2.6	+1.5	-2.2	-0.8	
7-layer CNN Standard/ Verified at 0% 73.8/55.4		Hydra	69.2	47.6	56.3	42.8	
		FaShapley	69.8	48.0	67.2	47.8	
		VeriSparse	73.9	56.8	70.7	52.7	
		Δ	+4.1	+8.8	+3.5	+5.7	

Table 2: Standard and Verified Accuracy for 4-layer CNN and 7-layer CNN trained for CIFAR-10 and SVHN at perturbation budget $2/255$ at different sparsity amounts obtained using unstructured pruning. Δ represents the change than the best baseline.

comparison is shown for two architectures: 4-layer CNN and 7-layer CNN trained for CIFAR-10 and SVHN. The perturbation amount used in these evaluations is $2/255$. Notably, on average, **VeriSparse** achieves comparable *Standard* accuracy and an average increment of 2.69% *Verified* accuracy than the best-baseline, when computed across all model, dataset, and sparsity combinations.

Table 3 compares the unstructured-pruned sparse models obtained at a higher perturbation budget, $8/255$. The evaluation shown for 4-layer CNN trained for CIFAR-10 at 95% and 99% sparsities suggests that sparse models obtained using **VeriSparse** exhibit *Standard* and *Verified* accuracy comparable to the best-baseline FaShapley [23].

This section’s evaluations establish that **VeriSparse** can obtain sparse NNs from scratch exhibiting similar performance on unstructured-pruned and significantly higher performance on structured-pruned sparsified architectures as compared to the *train-and-sparsify* mechanism-based best-baseline FaShapley. The performance here refers to *Standard* and *Verified* accuracy.

Sparsity	95%		99%	
	Standard	verified	standard	verified
Hydra	30.3	24.3	25.9	20.3
FaShapley	36.8	26.2	36.2	26.1
VeriSparse	38.8	27.6	35.9	26.6
Δ	+2.0	+1.4	-0.3	+0.5

Table 3: Standard and Verified Accuracy for 4-layer for CIFAR-10 at perturbation budget $8/255$ at different sparsity amounts obtained using unstructured pruning. The standard and verified accuracy of the dense model are 40.1 and 28.5, respectively.

4.2 Establishing the generalizability of **VeriSparse**

This section demonstrates the applicability and generalizability of **VeriSparse** by evaluating various *backbone network* (Section 3) architectures, complexities, and datasets from different domains. Evaluation results are discussed below:

Model	Resnet		DenseNet		ResNeXt	
	0%	99%	0%	99%	0%	99%
Standard	46.4	43.7	36.3	36.6	31.2	35.2
Verified	31.4	28.6	28.8	27.2	24.9	27.6

Table 4: Comparison of sparse models obtained using **VeriSparse**’s unstructured pruning for Resnet, DenseNet and ResNeXt trained for CIFAR-10 at perturbation budget $8/288$ and 99% sparsity with their dense counterparts.

Model	Resnet		DenseNet		ResNeXt	
	0%	90%	0%	90%	0%	90%
Standard	57.2	42.0	57.7	46.1	54.5	45.8
Verified	46.0	34.0	46.8	37.0	44.7	37.2

Table 5: Comparison of sparse models obtained using **VeriSparse**’s structured approach for Resnet, DenseNet and ResNeXt trained for CIFAR-10 at perturbation budget $2/288$ at 90% sparsity with their dense counterparts.

- **Evaluation for complex models:** To demonstrate the scalability and generalizability of **VeriSparse** to more complex backbone network architectures (hence, to compare with complex/dense counterparts), we compute sparse models for Resnet, DenseNet, and ResNext (used by [69]) on CIFAR-10 dataset at the maximum perturbation amounts shown in literature [75, 69], that is, $8/255$. Table 4 demonstrates that the unstructured-pruned sparse models obtained using **VeriSparse** having only 1% (at 99% sparsity) of the original parameters exhibit *Standard* and *Verified* accuracy comparable to the dense models having same backbone architecture.

For structured-pruned sparse models, we use smaller perturbation amount used in the baseline literature [23], that is $2/255$. Table 5 shows the evaluations for Resnet, DenseNet and ResNext trained for CIFAR-10 at 0% (dense) and 90% sparsity. **VeriSparse** extracted sparse networks’ performance in comparison to their dense counterparts is comparable to the Table 1 evaluation results, showing **VeriSparse**’s structured pruning mechanism performs similarly across different network complexities and architectures.

- **Application to sequential model:** To further investigate the application of **VeriSparse** to sequential networks, we evaluated a small LSTM [69] as a backbone architecture to obtain sparse models for MNIST. Table 6 demonstrates the *Standard* and *Verified* accuracy for the unstructured-pruned sparse models obtained using **VeriSparse**. It can be noted that up to 95% sparsity

Sparsity \Rightarrow	0%	80%	90%	95%	99%
Standard	96.0	95.6	95.7	94.5	88.5
Verified	85.8	88.2	89.3	86.1	81.3

Table 6: Comparison of sparse models obtained using **VeriSparse** for LSTM trained for MNIST at various sparsity amounts

amount, the sparse models’ *generalizability* are comparable to their dense counterparts. Additionally, higher error at 99% sparsity can be attributed to insufficient active-parameters for the target task.

Dataset	Pedestrian Detection			MNIST		
	0%	95%	99%	0%	95%	99%
Standard	71.6	73.8	71.6	97.7	96.7	97.9
Verified	36.5	32.7	37.0	87.8	85.5	88.0

Table 7: Comparison sparse models obtained using **VeriSparse** using 7-layer CNN as backbone architecture trained for (a) Pedestrian Detection and (b) MNIST at perturbations 2/255 and 0.4, respectively

Sparsity \Rightarrow	0%	80%	90%	95%	99%
Standard	79.1	79.8	77.8	78.9	78.5
Verified	75.7	77.7	76.1	76.5	76.3

Table 8: Comparison of sparse models obtained using **VeriSparse** using LSTM as the backbone architecture trained for SST-2 at different sparsity amounts

• **Evaluations for more datasets and domains:** This section evaluates **VeriSparse**’s generalizability on various datasets from image (MNIST and Pedestrian Detection) and non-image (SST-2 for sentiment analysis) domains.

Table 7 demonstrates the results for additional image datasets: (a) a pedestrian detection dataset that aims at differentiating between people and people-like objects [37], and (b) MNIST. The backbone architecture used for these evaluations is a 7-layer CNN, adapted to the respective datasets. For both datasets, the performance of the unstructured-pruned sparse models are comparable to that of their dense counterparts (i.e., 0% sparsity). The perturbation amount used for Pedestrian Detection and MNIST are 2/255, and 0.4.

For the Sentiment Analysis dataset SST-2, the perturbations are introduced in terms of synonym-based word substitution in a sentence, and the number of words substituted is called the *budget* δ . The value of δ used in the empirical analysis is 6.

Notably, this training does not use ℓ_p -norm perturbation, but to keep the perturbation amount continuous, the training procedure consists of an initial warm-up phase [69]. If the word at index i for a clean sentence and a perturbed sentence is represented by w_i and \hat{w}_i , and $e(w)$ is the embedding for the word w , the effective embedding used during training is given by:

$$e(w_i) = \epsilon * e(\hat{w}_i) + (1 - \epsilon) * e(w_i)$$

The value of ϵ is gradually increased from 0 to 1 during the training phase. The results thus produced for the original dense model (sparsity = 0%) are in compliance with state-of-the-art [69]. Table 8 shows that the sparse models obtained at different compression amounts using the presented approach exhibit *standard* and *verified* accuracy comparable to the original dense model.

4.3 Evaluation on Training and Inference Resource Reduction

This section evaluates the training and inference time, and resource reduction through the **VeriSparse** extracted sparse NNs, compared to their dense counterparts and baselines.

4.3.1 Reduction in Training Time for **VeriSparse**’s Sparse Network Extraction Compared to the Baselines:

VeriSparse requires almost one-third of clock-time as that of the *train-and-sparsify* mechanism based baselines [52, 23]. Table 9 compares the training time required by Hydra [52], FaShapley [23] and **VeriSparse** for 4-layer CNN and 7-layer CNN at 99% sparsity, while using the same number of training epochs. That is, the total number of epochs used in pre-training, pruning, and fine-tuning for state-of-the-art [52, 23] and an equal number of epochs for **VeriSparse**. Notably, in Table 2’s presented evaluations, the same number of epochs are utilized. These training times are computed for NVIDIA RTX A6000.

Method \Rightarrow	Hydra	FaShapely	VeriSparse
Model			
4-layer CNN	9.2	9.0	3.4
7-layer CNN	20.9	18.8	7.5

Table 9: Training Time (in Ksec) for Hydra, FaShapley and VeriSparse

4.3.2 Real-deployment Evaluations on the Reduction in Time and Memory Requirement of the Structured-pruned Sparse Models:

VeriSparse’s structured-pruned sparse models result in memory and inference time reductions in the resource constraint platforms. Table 10 compares sparse models with their dense counterparts on Google Pixel 6, which has 8GB RAM, powered by a 2.8GHz octa-core Google Tensor processor, running on an Android 12.0 system.

The inference time shown in Table 10 is computed as the average over the result of three experiment trials, which computes the average time required per sample over 10,000 repetitions. It is observed that 7-layer CNN and Resnet at 90% sparsity require about 5 – 8 times less memory, 2 – 5 times less inference time, and significantly less RAM used by their dense counterparts. These evaluations demonstrate the impact of VeriSparse in enabling resource-constraint platforms such as embedded systems to leverage

Model	Compression \Rightarrow	0%	90%
7-layer CNN	Inference Time(ms)	6.4	3.5
	Memory(MB)	68.8	13.7
	Peak CPU usage (%)	55	51
	Peak RAM usage(Mb)	98	60
Resnet	Inference Time(ms)	4.54	0.81
	Memory(MB)	16.9	2.07
	Peak CPU usage(%)	54	51
	Peak RAM usage(Mb)	50	37

Table 10: Comparison of inference time per sample and resource requirements for structured-pruned sparse models for 7-layer CNN and Resnet trained for CIFAR-10 with their dense counterparts on Google Pixel 6 verified robust models.

4.3.3 Reduction in inference time and Theoretical Analysis of FLOPs for the Unstructured-pruned Sparse Models:

Several works have shown that the models obtained using unstructured pruning approaches do not reduce inference time on generic computation platforms [46, 43]. This is so because the unstructured pruning approaches replace the removed network parameter values with zero while keeping the network structure intact. However, hardware such as NVIDIA RTX A6000 is optimized to explore fine-grained sparsity to speed up the standard Tensor Core operations [40]. We observe that the inference time of the unstructured-pruned sparse models obtained via VeriSparse is *five times* lesser, on average, than their dense counterparts on NVIDIA RTX A6000. The computation times shown in Table 11 are computed for the CIFAR-10 dataset for three models: 4-layer CNN, 7-layer CNN and Resnet at different sparsity amounts, and the inference times are calculated as an average over 10000 repetitions.

The reduction in computation during the inferences of sparse models can be attributed to a decrease in the number of Floating Point Operations (FLOPs). To compute the theoretical reduction in the number of FLOPs, the standard Tensor operation for each layer is scaled by the number of zeroed-out parameters, the metric defined by Blalock et al. [4]. Table 12 compares the FLOPs for dense and unstructured-pruned sparse models for 4-layer CNN, 7-layer CNN, and Resnet trained for CIFAR-10. It can be observed that the sparse models required lesser FLOPs as compared to the dense models (sparsity = 0%). The Flops are computed using the code in git repository [3].

4.4 VeriSparse Self-Learns the Sparse Architecture and Parameters

The dynamic masking used by VeriSparse allows for learning sparse structures alongside parameter weights, facilitating the effective minimization of the training loss, i.e., identification of sparse network with high verified local robustness. This section visualizes such sparse architecture extraction while performing the unstructured pruning mechanism of VeriSparse by showing the evolution of per-layer pruning/sparsification amounts in the backbone network.

Compression \Rightarrow Model	0%	95%	99%
4-layer CNN	1.8×10^{-5}	7.5×10^{-6}	6.4×10^{-6}
7-layer CNN	1.1×10^{-4}	1.8×10^{-5}	1.7×10^{-5}
Resnet	1.1×10^{-4}	2.9×10^{-5}	2.8×10^{-5}

Table 11: Inference Time (in sec) for unstructured-pruned sparse models on NVIDIA RTX A6000 at different sparsity amounts

Compression \Rightarrow Model	0%	95%	99%
4-layer CNN	494.08	27.42	16.98
7-layer CNN	150672.38	15311.38	7433.213
Resnet	24471312.0	4052061.0	2366837.0

Table 12: Effective FLOPs (in KMacs) for unstructured sparse models at different sparsity amounts

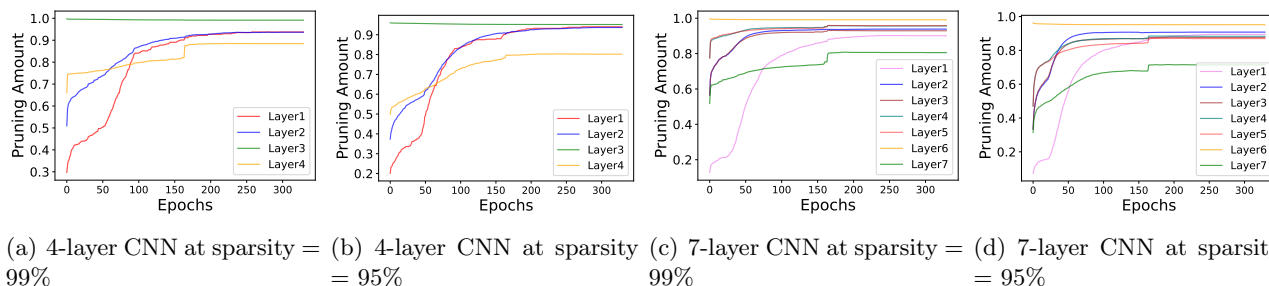


Figure 3: Adaptive layer-wise pruning amounts at global sparsity of 99% and 95% for a 4-layer CNN and 7-layer CNN trained for CIFAR-10 dataset

Figure 3 shows the changes in the per-layer pruning/sparsification amounts on the backbone networks: 4-layer CNN and 7-layer CNN trained for CIFAR-10 at 99% and 95% sparsity. An important observation here is that at both the sparsity amounts, the final per-layer pruning amounts (i.e., identified sparse network structure) follow the same pattern. The last layer, i.e., the decision-making layer, is pruned the least, followed by the initial layers (e.g., 1, 2), which are the initial feature extraction layers. The Layer before the last is pruned the most, which is a large linear layer containing the most number of network parameters. Notably, Sanh et al. [48] observed similar patterns on the sparse models extracted through global magnitude-based *train-and-sparsify* sparsification. Such networks, too, tend to have low sparsity on the earlier layers due to their higher importance in feature extraction. *Such similarity demonstrates VeriSparse’s ability to identify effective sparse network structures.*

In the Figure 3’s backbone dense networks, the initial feature-extracting convolution layers have significantly fewer parameters than the latter dense linear layers, so even a small change in their active/dormant parameters results in a bigger fractional change. As evident from Figure 3, the increment in the initial layers’ dormant parameters is compensated by a small fractional reduction in the latter layers. To recall, fraction of parameters which are dormant is the current sparsity.

Notably, *the per-layer pruning amount stabilizes around halfway through the training, indicating the identification of the sparse structure. After that, the parameter weights of the identified sparse network are optimized to minimize the training loss.* These visualizations demonstrate VeriSparse’s dynamic exploration of network structure and parameters through sparse training that results in effective sparse architectures with high verified local robustness.

5 Discussion on Impact and Limitations

Impact: Deploying and training neural network (NN) models in embedded systems are considered challenging because of limited resources such as memory, processing, and energy capacity [57, 72]. Such constraints cause latency in the training and inference generation of NN models, which limits embedded systems’ use in edge and time-critical applications [57]. The evaluations presented in Section 4.3 suggest that alongside introducing high verified local robustness in the NN models, the VeriSparse addresses the issues mentioned above in the embedded systems:

- VeriSparse enables the extraction of structured-pruned sparse networks with high verified local robustness. Such sparse models require significantly less storage and RAM than their dense counterparts, addressing embedded systems’ memory constraint challenge.
- Notably, the training time of the VeriSparse approach is 2 – 3 times less than the baseline approaches. Implying that it reduces the training latency and processing need, thus, increasing the feasibility of NN training in the embedded edge platforms.
- The structured-pruned sparse models extracted through VeriSparse require significantly less inference time, storage, and RAM on the resource-constraint platform. Thus, VeriSparse represents a significant advancement in the development of efficient, accurate, and verified robust neural networks that can be deployed in safety-critical and real-time resource-constrained environments.

Limitations & future-works:

- VeriSparse uses CROWN-IBP; thus, its efficacy is restricted by the robustness achieved by CROWN-IBP. However, with the advancement of LiRPA-based verification approaches, newer/advanced

bounding mechanisms can be adapted in **VeriSparse**, enabling higher verified local robustness.

- There is rich literature on pruning. However, we only investigated global unstructured and layer-wise structured pruning mechanisms in the *Pruning Phase* of **VeriSparse** (Section 3.3.3); it is due to a fair comparison with the baselines. Also, to demonstrate that leveraging the most common pruning mechanisms, it is possible to obtain a sparse network from scratch comparable in verified local robustness to the train-and-sparsify-based sparsification baselines [52, 23].

- Finally, following most studies in literature, this paper addresses up to 99% model sparsification. However, our analysis shows that *generalizability* decreases on extreme sparsity (99.9%). E.g., at 99.9% sparsity, the 7-layer CNN exhibits a reduction of approximately 7% in *standard accuracy* and 10% in *verified accuracy* for both MNIST and CIFAR-10 datasets. This suggests that an optimal sparsity exists in the range of (99% - 99.9%) at which the sparse model generalizes comparable to its dense counterpart. Though finding optimal sparsity is out of scope, future work on this scope would be beneficial.

6 Conclusion

This is the first work showing that a verified locally robust sparse network is trainable from scratch, leveraging a dynamic-mask-based mechanism. The ability to train a sparse network from scratch renders the conventional requirement of training a dense network nonobligatory and significantly reduces the training time. Presented evaluations show **VeriSparse**'s superior performance in identifying *higher verified locally robust* sparse neural networks compared to the state-of-the-art baselines. Presented extensive evaluations demonstrate that **VeriSparse** significantly reduces storage, computing-resource, and computation time and is generalizable to various network architectures, complexities, and dataset domains. Thus, it enables the deployment and training of *verified locally robust* NN models in resource-constrained safety-critical and real-time systems.

References

- [1] T. Akiba, S. Sano, T. Yanase, T. Ohta, and M. Koyama. 2019. Optuna: A Next-generation Hyperparameter Optimization Framework.
- [2] Ron Banner, Itay Hubara, Elad Hoffer, and Daniel Soudry. 2018. Scalable methods for 8-bit training of neural networks. In *Advances in Neural Information Processing Systems*, S. Bengio, H. Wallach, H. Larochelle, K. Grauman, N. Cesa-Bianchi, and R. Garnett (Eds.), Vol. 31. Curran Associates, Inc.
- [3] Davis Blalock, Jose Javier Gonzalez Ortiz, Jonathan Frankle, and John Gutttag. 2020. ShrinkBench. <https://github.com/jjgo/shrinkbench>.
- [4] Davis Blalock, Jose Javier Gonzalez Ortiz, Jonathan Frankle, and John Gutttag. 2020. What is the State of Neural Network Pruning? arXiv:2003.03033 [cs.LG]
- [5] X. Dai, H. Yin, and N. K. Jha. 2019. NeST: A Neural Network Synthesis Tool Based on a Grow-and-Prune Paradigm. *IEEE Trans. Comput.* 68, 10 (oct 2019), 1487–1497. <https://doi.org/10.1109/TC.2019.2914438>
- [6] Tim Dettmers and Luke Zettlemoyer. 2019. Sparse Networks from Scratch: Faster Training without Losing Performance. <https://doi.org/10.48550/ARXIV.1907.04840>
- [7] Thomas Elsken, Jan Hendrik Metzen, and Frank Hutter. 2019. Neural Architecture Search: A Survey. *J. Mach. Learn. Res.* 20, 1 (jan 2019), 1997–2017.
- [8] Utku Evci, Yani Ioannou, Cem Keskin, and Yann Dauphin. 2022. Gradient Flow in Sparse Neural Networks and How Lottery Tickets Win. *Proceedings of the AAAI Conference on Artificial Intelligence* 36, 6 (Jun. 2022), 6577–6586. <https://doi.org/10.1609/aaai.v36i6.20611>

-
- [9] Gongfan Fang, Xinyin Ma, Mingli Song, Michael Bi Mi, and Xinchao Wang. 2023. DepGraph: Towards Any Structural Pruning. arXiv:2301.12900 [cs.AI]
- [10] Jonathan Frankle and Michael Carbin. 2019. The Lottery Ticket Hypothesis: Finding Sparse, Trainable Neural Networks. In *International Conference on Learning Representations*.
- [11] Jonathan Frankle, Gintare Karolina Dziugaite, Daniel Roy, and Michael Carbin. 2020. Linear mode connectivity and the lottery ticket hypothesis. In *International Conference on Machine Learning*. PMLR, 3259–3269.
- [12] Aymeric Fromherz, Klas Leino, Matt Fredrikson, Bryan Parno, and Corina Pasareanu. 2021. Fast Geometric Projections for Local Robustness Certification. In *International Conference on Learning Representations*.
- [13] Ian J. Goodfellow, Jonathon Shlens, and Christian Szegedy. 2015. Explaining and Harnessing Adversarial Examples. *CoRR* abs/1412.6572 (2015).
- [14] Sven Gowal, Krishnamurthy Dvijotham, Robert Stanforth, Rudy Bunel, Chongli Qin, Jonathan Uesato, Relja Arandjelovic, Timothy Mann, and Pushmeet Kohli. 2018. On the Effectiveness of Interval Bound Propagation for Training Verifiably Robust Models. <https://doi.org/10.48550/ARXIV.1810.12715>
- [15] Song Han, Xingyu Liu, Huizi Mao, Jing Pu, Ardavan Pedram, Mark A. Horowitz, and William J. Dally. 2016. EIE: Efficient Inference Engine on Compressed Deep Neural Network. <https://doi.org/10.48550/ARXIV.1602.01528>
- [16] Song Han, Xingyu Liu, Huizi Mao, Jing Pu, Ardavan Pedram, Mark A. Horowitz, and William J. Dally. 2016. EIE: Efficient Inference Engine on Compressed Deep Neural Network. *SIGARCH Comput. Archit. News* 44, 3 (jun 2016), 243–254. <https://doi.org/10.1145/3007787.3001163>
- [17] Juncai He, Xiaodong Jia, Jinchao Xu, Lian Zhang, and Liang Zhao. 2020. Make L1 regularization effective in training sparse CNN. *Computational Optimization and Applications* 77, 1 (1 sep 2020), 163–182. <https://doi.org/10.1007/s10589-020-00202-1>
- [18] Yang He, Guoliang Kang, Xuanyi Dong, Yanwei Fu, and Yi Yang. 2018. Soft Filter Pruning for Accelerating Deep Convolutional Neural Networks. arXiv:1808.06866 [cs.CV]
- [19] Geoffrey Hinton, Jeff Dean, and Oriol Vinyals. 2014. Distilling the Knowledge in a Neural Network. 1–9.
- [20] Torsten Hoeffler, Dan Alistarh, Tal Ben-Nun, Nikoli Dryden, and Alexandra Peste. 2021. Sparsity in Deep Learning: Pruning and Growth for Efficient Inference and Training in Neural Networks. *J. Mach. Learn. Res.* 22, 1, Article 241 (jan 2021), 124 pages.
- [21] Robin Jia, Aditi Raghunathan, Kerem Göksel, and Percy Liang. 2019. Certified Robustness to Adversarial Word Substitutions. <https://doi.org/10.48550/ARXIV.1909.00986>
- [22] Artur Jordao and Helio Pedrini. 2021. On the Effect of Pruning on Adversarial Robustness. <https://doi.org/10.48550/ARXIV.2108.04890>
- [23] Mintong Kang, Linyi Li, and Bo Li. 2023. FaShapley: Fast and Approximated Shapley Based Model Pruning Towards Certifiably Robust DNNs. In *First IEEE Conference on Secure and Trustworthy Machine Learning*. https://openreview.net/forum?id=mJF9_Fs52ut
- [24] Guy Katz, Clark Barrett, David L. Dill, Kyle Julian, and Mykel J. Kochenderfer. 2017. Reluplex: An Efficient SMT Solver for Verifying Deep Neural Networks. In *Computer Aided Verification*, Rupak Majumdar and Viktor Kunčák (Eds.). Springer International Publishing, 97–117.
- [25] Alex Krizhevsky, Vinod Nair, and Geoffrey Hinton. 2009. Learning multiple layers of features from tiny images. (2009).

- [26] Alexey Kurakin, Ian Goodfellow, and Samy Bengio. 2016. Adversarial examples in the physical world. <https://doi.org/10.48550/ARXIV.1607.02533>
- [27] Yann LeCun and Corinna Cortes. 2010. MNIST handwritten digit database. <http://yann.lecun.com/exdb/mnist/>. (2010). <http://yann.lecun.com/exdb/mnist/>
- [28] Byung-Kwan Lee, Junho Kim, and Yong Man Ro. 2022. Masking Adversarial Damage: Finding Adversarial Saliency for Robust and Sparse Network. In *Proceedings of the IEEE/CVF Conference on Computer Vision and Pattern Recognition (CVPR)*. 15126–15136.
- [29] Byung-Kwan Lee, Junho Kim, and Yong Man Ro. 2022. Masking Adversarial Damage: Finding Adversarial Saliency for Robust and Sparse Network. arXiv:2204.02738 [cs.CV]
- [30] Hao Li, Asim Kadav, Igor Durdanovic, Hanan Samet, and Hans Peter Graf. 2017. Pruning Filters for Efficient ConvNets. *ArXiv* abs/1608.08710 (2017).
- [31] Lucas Liebenwein, Cenk Baykal, Brandon Carter, David Gifford, and Daniela Rus. 2021. Lost in Pruning: The Effects of Pruning Neural Networks beyond Test Accuracy. <https://doi.org/10.48550/ARXIV.2103.03014>
- [32] Shiwei Liu, Lu Yin, Decebal Constantin Mocanu, and Mykola Pechenizkiy. 2021. Do We Actually Need Dense Over-Parameterization? In-Time Over-Parameterization in Sparse Training. In *Proceedings of the 38th International Conference on Machine Learning (Proceedings of Machine Learning Research, Vol. 139)*, Marina Meila and Tong Zhang (Eds.). PMLR, 6989–7000.
- [33] Christos Louizos, Max Welling, and Diederik P. Kingma. 2018. Learning Sparse Neural Networks through L0 Regularization. In *International Conference on Learning Representations*. <https://openreview.net/forum?id=H1Y8hhg0b>
- [34] Zhaoyang Lyu, Ching-Yun Ko, Zhifeng Kong, Ngai Wong, Dahua Lin, and Luca Daniel. 2020. Fastened CROWN: Tightened Neural Network Robustness Certificates. *ArXiv* abs/1912.00574 (2020).
- [35] Pavlo Molchanov, Stephen Tyree, Tero Karras, Timo Aila, and Jan Kautz. 2017. Pruning Convolutional Neural Networks for Resource Efficient Inference. In *5th International Conference on Learning Representations, ICLR 2017, Toulon, France, April 24-26, 2017, Conference Track Proceedings*. OpenReview.net. <https://openreview.net/forum?id=SJGCiw5gl>
- [36] Pavlo Molchanov, Stephen Tyree, Tero Karras, Timo Aila, and Jan Kautz. 2017. Pruning Convolutional Neural Networks for Resource Efficient Inference. In *5th International Conference on Learning Representations, ICLR 2017, Toulon, France, April 24-26, 2017, Conference Track Proceedings*. OpenReview.net. <https://openreview.net/forum?id=SJGCiw5gl>
- [37] Chandran Saravanan N J Karthika. 2020. Addressing False Positives in Pedestrian Detection. In *International Conference on Electronic Systems and Intelligent Computing (ESIC 2020)*. https://doi.org/10.1007/978-981-15-7031-5_103
- [38] Sharan Narang, Greg Diamos, Shubho Sengupta, and Erich Elsen. 2017. Exploring Sparsity in Recurrent Neural Networks. In *International Conference on Learning Representations*. <https://openreview.net/forum?id=BylSPv9gx>
- [39] Yuval Netzer, Tao Wang, Adam Coates, Alessandro Bissacco, Bo Wu, and Andrew Y. Ng. 2011. Reading Digits in Natural Images with Unsupervised Feature Learning. In *NIPS Workshop on Deep Learning and Unsupervised Feature Learning 2011*. http://ufldl.stanford.edu/housenumbers/nips2011_housenumbers.pdf
- [40] NVIDIA. 2022. NVIDIA RTX A6000 Graphics Card. <https://www.nvidia.com/en-us/design-visualization/rtx-a6000/>

-
- [41] Ana Pereira and Carsten Thomas. 2020. Challenges of Machine Learning Applied to Safety-Critical Cyber-Physical Systems. *Machine Learning and Knowledge Extraction* 2, 4 (2020), 579–602. <https://doi.org/10.3390/make2040031>
- [42] Huy Phan, Miao Yin, Yang Sui, Bo Yuan, and Saman Zonouz. 2022. CSTAR: Towards Compact and STructured Deep Neural Networks with Adversarial Robustness. <https://doi.org/10.48550/arXiv.2212.01957>
- [43] Oleg Polivin. 2020. Experiments in Neural Network Pruning (in PyTorch). <https://olegpolivin.medium.com/experiments-in-neural-network-pruning-in-pytorch-c18d5b771d6d>.
- [44] Pytorch. 2019. PRUNING TUTORIAL. https://pytorch.org/tutorials/intermediate/pruning_tutorial.html#pruning-tutorial.
- [45] Pytorch. 2020. Global structured pruning. <https://discuss.pytorch.org/t/global-structured-pruning/67263>.
- [46] Isma-Ilou Sadou, Seyed Morteza Nabavinejad, Zhonghai Lu, and Masoumeh Ebrahimi. 2022. Inference Time Reduction of Deep Neural Networks on Embedded Devices: A Case Study. In *2022 25th Euromicro Conference on Digital System Design (DSD)*. 205–213. <https://doi.org/10.1109/DSD57027.2022.00036>
- [47] Tara N. Sainath, Brian Kingsbury, Vikas Sindhvani, Ebru Arisoy, and Bhuvana Ramabhadran. 2013. Low-rank matrix factorization for Deep Neural Network training with high-dimensional output targets. In *2013 IEEE International Conference on Acoustics, Speech and Signal Processing*. 6655–6659. <https://doi.org/10.1109/ICASSP.2013.6638949>
- [48] Victor Sanh, Thomas Wolf, and Alexander M. Rush. 2020. Movement Pruning: Adaptive Sparsity by Fine-Tuning. <https://doi.org/10.48550/ARXIV.2005.07683>
- [49] Abigail See, Minh-Thang Luong, and Christopher D. Manning. 2016. Compression of Neural Machine Translation Models via Pruning. <https://doi.org/10.48550/ARXIV.1606.09274>
- [50] Abigail See, Minh-Thang Luong, and Christopher D. Manning. 2016. Compression of Neural Machine Translation Models via Pruning. In *Proceedings of the 20th SIGNLL Conference on Computational Natural Language Learning*. Association for Computational Linguistics, Berlin, Germany, 291–301. <https://doi.org/10.18653/v1/K16-1029>
- [51] Vikash Sehwal, Shiqi Wang, Prateek Mittal, and Suman Jana. 2019. Towards Compact and Robust Deep Neural Networks. *preprint arXiv:1906.06110* (2019). arXiv:1906.06110 [cs.LG]
- [52] Vikash Sehwal, Shiqi Wang, Prateek Mittal, and Suman Jana. 2020. HYDRA: Pruning Adversarially Robust Neural Networks. *34th Conference on Neural Information Processing Systems (NeurIPS 2020)* (2020).
- [53] Gagandeep Singh, Timon Gehr, Markus Püschel, and Martin Vechev. 2019. An Abstract Domain for Certifying Neural Networks. *Proc. ACM Program. Lang.* 3, POPL, Article 41 (jan 2019), 30 pages. <https://doi.org/10.1145/3290354>
- [54] Sidak Pal Singh and Dan Alistarh. 2020. WoodFisher: Efficient Second-Order Approximation for Neural Network Compression. In *Advances in Neural Information Processing Systems*, H. Larochelle, M. Ranzato, R. Hadsell, M.F. Balcan, and H. Lin (Eds.), Vol. 33. Curran Associates, Inc., 18098–18109.
- [55] Aman Sinha, Hongseok Namkoong, and John Duchi. 2018. Certifiable Distributional Robustness with Principled Adversarial Training. In *International Conference on Learning Representations*.

- [56] Richard Socher, Alex Perelygin, Jean Wu, Jason Chuang, Christopher D. Manning, Andrew Ng, and Christopher Potts. 2013. Recursive Deep Models for Semantic Compositionality Over a Sentiment Treebank. In *Proceedings of the 2013 Conference on Empirical Methods in Natural Language Processing*. Association for Computational Linguistics, Seattle, Washington, USA, 1631–1642. <https://aclanthology.org/D13-1170>
- [57] Bluefruit Software. 2021. Machine learning and embedded systems: exploring the relationship. <https://www.bluefruit.co.uk/quality/machine-learning-embedded-systems-relationship/>.
- [58] Ghada Sokar, Elena Mocanu, Decebal Constantin Mocanu, Mykola Pechenizkiy, and Peter Stone. 2022. Dynamic Sparse Training for Deep Reinforcement Learning. arXiv:2106.04217 [cs.LG]
- [59] Chong Min John Tan and Mehul Motani. 2020. DropNet: Reducing Neural Network Complexity via Iterative Pruning. In *Proceedings of the 37th International Conference on Machine Learning (Proceedings of Machine Learning Research, Vol. 119)*, Hal Daumé III and Aarti Singh (Eds.). PMLR, 9356–9366.
- [60] Hugo Tessier. 2021. Neural Network Pruning 101. <https://towardsdatascience.com/neural-network-pruning-101-af816aaea61>.
- [61] Vincent Tjeng, Kai Y. Xiao, and Russ Tedrake. 2019. Evaluating Robustness of Neural Networks with Mixed Integer Programming. In *International Conference on Learning Representations*.
- [62] Chaoqi Wang, Guodong Zhang, and Roger Grosse. 2020. Picking Winning Tickets Before Training by Preserving Gradient Flow. In *International Conference on Learning Representations*. <https://openreview.net/forum?id=SkgsACVKPH>
- [63] Shiqi Wang, Huan Zhang, Kaidi Xu, Xue Lin, Suman Jana, Cho-Jui Hsieh, and J Zico Kolter. 2021. Beta-CROWN: Efficient Bound Propagation with Per-neuron Split Constraints for Neural Network Robustness Verification. In *Advances in Neural Information Processing Systems*, A. Beygelzimer, Y. Dauphin, P. Liang, and J. Wortman Vaughan (Eds.).
- [64] Yisen Wang, Difan Zou, Jinfeng Yi, James Bailey, Xingjun Ma, and Quanquan Gu. 2020. Improving Adversarial Robustness Requires Revisiting Misclassified Examples. In *International Conference on Learning Representations*.
- [65] Lily Weng, Huan Zhang, Hongge Chen, Zhao Song, Cho-Jui Hsieh, Luca Daniel, Duane Boning, and Inderjit Dhillon. 2018. Towards Fast Computation of Certified Robustness for ReLU Networks. In *Proceedings of the 35th International Conference on Machine Learning (Proceedings of Machine Learning Research, Vol. 80)*, Jennifer Dy and Andreas Krause (Eds.). PMLR, 5276–5285. <https://proceedings.mlr.press/v80/weng18a.html>
- [66] Cody Marie Wild. 2018. Know Your Adversary: Understanding Adversarial Examples (Part 1/2). <https://towardsdatascience.com/know-your-adversary-understanding-adversarial-examples-part-1-2-63af4c2f5830>.
- [67] Eric Wong and Zico Kolter. 2018. Provable Defenses against Adversarial Examples via the Convex Outer Adversarial Polytope. In *Proceedings of the 35th International Conference on Machine Learning (Proceedings of Machine Learning Research, Vol. 80)*, Jennifer Dy and Andreas Krause (Eds.). PMLR, 5286–5295.
- [68] Eric Wong, Frank Schmidt, Jan Hendrik Metzen, and J. Zico Kolter. 2018. Scaling provable adversarial defenses. In *Advances in Neural Information Processing Systems*, S. Bengio, H. Wallach, H. Larochelle, K. Grauman, N. Cesa-Bianchi, and R. Garnett (Eds.), Vol. 31. Curran Associates, Inc.

- [69] Kaidi Xu, Zhouxing Shi, Huan Zhang, Yihan Wang, Kai-Wei Chang, Minlie Huang, Bhavya Kaillkhura, Xue Lin, and Cho-Jui Hsieh. 2020. Automatic Perturbation Analysis for Scalable Certified Robustness and Beyond. In *Proceedings of the 34th International Conference on Neural Information Processing Systems (Vancouver, BC, Canada) (NIPS’20)*. Curran Associates Inc., Red Hook, NY, USA, Article 96.
- [70] Kaidi Xu, Huan Zhang, Shiqi Wang, Yihan Wang, Suman Jana, Xue Lin, and Cho-Jui Hsieh. 2021. Fast and Complete: Enabling Complete Neural Network Verification with Rapid and Massively Parallel Incomplete Verifiers. In *International Conference on Learning Representations*.
- [71] Kaidi Xu, Huan Zhang, Shiqi Wang, Yihan Wang, Suman Jana, Xue Lin, and Cho-Jui Hsieh. 2021. Fast and Complete: Enabling Complete Neural Network Verification with Rapid and Massively Parallel Incomplete Verifiers. In *International Conference on Learning Representations*.
- [72] Lei Xun, Long Tran-Thanh, Bashir M Al-Hashimi, and Geoff V. Merrett. 2021. Optimising Resource Management for Embedded Machine Learning. arXiv:2105.03608 [cs.CV]
- [73] S. Ye, K. Xu, S. Liu, H. Cheng, J. Lambrechts, H. Zhang, A. Zhou, K. Ma, Y. Wang, and X. Lin. 2019. Adversarial Robustness vs. Model Compression, or Both?. In *2019 IEEE/CVF International Conference on Computer Vision (ICCV)*. IEEE Computer Society, Los Alamitos, CA, USA, 111–120. <https://doi.org/10.1109/ICCV.2019.00020>
- [74] Zhonghui You, Kun Yan, Jinmian Ye, Meng Ma, and Ping Wang. 2019. Gate Decorator: Global Filter Pruning Method for Accelerating Deep Convolutional Neural Networks. <https://doi.org/10.48550/ARXIV.1909.08174>
- [75] Huan Zhang, Hongge Chen, Chaowei Xiao, Sven Gowal, Robert Stanforth, Bo Li, Duane S. Boning, and Cho-Jui Hsieh. 2020. Towards Stable and Efficient Training of Verifiably Robust Neural Networks. In *8th International Conference on Learning Representations, ICLR 2020, Addis Ababa, Ethiopia, April 26-30, 2020*. OpenReview.net.
- [76] Huan Zhang, Tsui-Wei Weng, Pin-Yu Chen, Cho-Jui Hsieh, and Luca Daniel. 2018. Efficient Neural Network Robustness Certification with General Activation Functions. *ArXiv* abs/1811.00866 (2018).
- [77] Jingfeng Zhang, Xilie Xu, Bo Han, Gang Niu, Lizhen Cui, Masashi Sugiyama, and Mohan Kankanhalli. 2020. Attacks Which Do Not Kill Training Make Adversarial Learning Stronger. In *Proceedings of the 37th International Conference on Machine Learning (Proceedings of Machine Learning Research, Vol. 119)*, Hal Daumé III and Aarti Singh (Eds.). PMLR, 11278–11287.
- [78] Tianyun Zhang, Shaokai Ye, Kaiqi Zhang, Jian Tang, Wujie Wen, Makan Fardad, and Yanzhi Wang. 2018. A systematic dnn weight pruning framework using alternating direction method of multipliers. In *Proceedings of the European Conference on Computer Vision (ECCV)*. 184–199.

A Using Different bounding mechanisms for verified local robustness

Table 13 compares the errors exhibited by 4-layer CNN at 99% sparsity when trained by employing different bounding mechanisms to compute $\mathcal{L}_{\text{train}}$: IBP [14], CROWN [76], Fastened-CROWN [34], and CROWN-IBP [75].

Dataset	Method \Rightarrow Error	IBP	CROWN	CROWN-Fast	CROWN-IBP
MNIST $\varepsilon = 0.4$	Standard	92.6	47.7	86.5	92.8
	Verified	78.5	6.9	57.8	78.0
CIFAR $\varepsilon = 8/255$	Standard	37.1	31.0	31.3	35.0
	Verified	21.5	11.7	10.6	26.6

Table 13: Comparison of different formal verification mechanism used to compute $\mathcal{L}_{\text{train}}$ on 4-layer CNN trained for MNIST and CIFAR-10 at 99% sparsity